Development 135, 2479-2488 (2008) doi:10.1242/dev.014902

Separating genetic and hemodynamic defects in neuropilin 1 knockout embryos

Elizabeth A. V. Jones[1,2,*], Li Yuan[3], Christine Breant[1,2], Ryan J. Watts[4] and Anne Eichmann[1,2]

Targeted inactivation of genes involved in murine cardiovascular development frequently leads to abnormalities in blood flow. As blood fluid dynamics play a crucial role in shaping vessel morphology, the presence of flow defects generally prohibits the precise assignment of the role of the mutated gene product in the vasculature. In this study, we show how to distinguish between genetic defects caused by targeted inactivation of the neuropilin 1 (Nrp1) receptor and hemodynamic defects occurring in homozygous knockout embryos. Our analysis of a *Nrp1* null allele bred onto a C57BL/6 background shows that vessel remodeling defects occur concomitantly with the onset of blood flow and cause death of homozygous mutants at E10.5. Using mouse embryo culture, we establish that hemodynamic defects are already present at E8.5 and continuous circulation is never established in homozygous mutants. The geometry of yolk sac blood vessels is altered and remodeling into yolk sac arteries and veins does not occur. To separate flow-induced deficiencies from those caused by the *Nrp1* mutation, we arrested blood flow in cultured wild-type and mutant embryos and followed their vascular development. We find that loss of Nrp1 function rather than flow induces the altered geometry of the capillary plexus. Endothelial cell migration, but not replication, is altered in *Nrp1* mutants. Gene expression analysis of endothelial cells isolated from freshly dissected wild-type and mutants and after culture in no-flow conditions showed down-regulation of the arterial marker genes connexin 40 and ephrin B2 related to the loss of *Nrp1* function. This method allows genetic defects caused by loss-of-function of a gene important for cardiovascular development to be isolated even in the presence of hemodynamic defects.

KEY WORDS: Neuropilin 1, VEGF, Hemodynamics, Endothelial cell migration, Arterial-venous differentiation

INTRODUCTION

The cardiovascular system is one of the few organ systems that must be functional as it develops. In mice, the embryonic heart forms as a linear tube at embryonic day 8 (E8.0) that must beat and supply blood flow before it has undergone looping, trabeculation or compartmentalization. The early blood vessels form as a capillary plexus in an extra-embryonic membrane called the yolk sac. Prior to the onset of heartbeat, this plexus is devoid of visible arteries or veins, and the vessels lack peripheral cell coverage. When blood first flows through the capillary plexus, the network is rapidly remodeled into a functional circulatory system composed of arteries, veins and capillaries. Structure and function develop in a coordinated manner and proper blood flow is required for normal cardiovascular development (Chapman, 1918; le Noble et al., 2004; Lucitti et al., 2007). If blood flow is stopped or is sufficiently abnormal, the blood vessels remain as a capillary plexus and do not undergo subsequent aspects of cardiovascular development. Therefore, the role of signaling molecules in the developing cardiovascular system is often obscured by the varied inputs of an organ system that has already begun to function.

In many cases, null mutations for genes required for proper vascular development also perturb proper blood flow. Genes that are expressed in the endothelium are most often also expressed in the endocardial lining of the heart, which could affect function. Irregularities in vascular geometry, such as occlusions or shunts, can also cause abnormal flow (Jones et al., 2004). Therefore, if a gene is important enough to visibly perturb cardiovascular structures, it will often perturb cardiovascular function as well. Over 50 genes have been published that cause a failure of yolk sac remodeling (Mary Dickinson, personal communication). Though improper blood flow can cause this phenotype, early circulatory function has been investigated in only a minority of these embryos. Vascular abnormalities present in the N-cadherin-null mouse can be rescued by restoring normal blood flow using cardiac-specific expression of either N- or E-cadherin (Luo et al., 2001), indicating that the observed vascular abnormalities are secondary to the abnormal blood flow. Abnormal or absent blood flow has been shown to cause failure to remodel in embryos (Lucitti et al., 2007), more cuboidal endothelial cell shape (May et al., 2004), vessel regression (Clark, 1918; Meeson et al., 1996; Thoma, 1893), abnormalities in peripheral cell recruitment (Grazioli et al., 2006) and changes in vessel diameter (Thoma, 1893). Proper vascular development requires a complex interaction of both genetic and physical signals, where one cannot develop normally without the other. It is therefore essential to separate when these events occur because of the mutation of interest and when they are induced by abnormal blood flow.

The neuropilin 1 (Nrp1) receptor was originally identified as a receptor for the axon guidance molecule semaphorin 3A and is implicated in the development of the nervous system (He and Tessier-Lavigne, 1997; Kolodkin et al., 1997). Nrp1 is also an isoform-specific receptor for $VEGF_{165}$ (Soker et al., 1998) and plays an important role in the cardiovascular system, as deletion of the *Nrp1* gene leads to embryonic lethality due to cardiovascular malformations. Lethality occurs between E10.5 and E13.5, depending on the genetic background (Kitsukawa et al., 1997). On a CD1 background, embryos lacking *Nrp1* exhibit defects in the formation of the heart outflow tract and aortic arches (Kawasaki et

[1]INSERM U833, F-75005, Paris, France. [2]Collège de France, 11 Place Marcelin Berthelot, 75005 Paris, France. [3]School of Life Science, Xiamen University 361005 Xiamen, Fujian, China. [4]Department of Tumor Biology and Angiogenesis, Genentech, 1 DNA Way, South San Francisco, CA 94080, USA.

*Author for correspondence (e-mail: liz.jones@mcgill.ca)

Accepted 15 May 2008

al., 1999). In addition, they exhibit abnormal vascular network formation in the yolk sac (Kawasaki et al., 1999) and abnormal sprouting of hindbrain vessels (Gerhardt et al., 2004). Furthermore, in endothelial-specific *Nrp1* knockouts, certain arterial markers are missing from arterioles and arteries (Mukouyama et al., 2005). The presence of both cardiac and vascular defects indicated that *Nrp1*-null embryos could present abnormal blood flow patterns and that aspects of their phenotype could be induced by improper flow rather than by loss of function of the receptor. We therefore decided to examine flow patterns in relation to vascular defects in these embryos.

We investigate here the cardiovascular phenotype of a *Nrp1* mutant allele (Gu et al., 2003) bred on a C57BL/6 background. $Nrp1^{-/-}$ embryos die at E10.5 with severe vascular abnormalities that are accompanied by abnormal flow patterns. In order to separate flow-induced defects from defects induced by the *Nrp1* mutation, we compared wild-type and mutant embryos in the absence of flow. We find that the yolk-sac vascular defects are not related to the flow defect but are due to loss of Nrp1 function. Function-blocking anti-Nrp1 antibodies (Pan et al., 2007a) injected into wild-type embryos can reproduce the yolk sac vessel defects observed in *Nrp1* mutants in a normal flow environment. By identifying an aspect of the mutant phenotype that is not dependent on flow, we are then able to investigate the genetic causes of this defect. We find that $Nrp1^{-/-}$ endothelial cells exhibit normal replication, but altered migration and defective arterial differentiation.

MATERIALS AND METHODS

Mice

Nrp1 mutant mice on a C57BL/6 background were generated as described (Gu et al., 2003). Briefly, a conditional targeted allele contained two *loxP* sites flanking exon 2 of the *Nrp1* gene was created. *Nrp1*-null mice were obtained by crossing mice harboring this conditional allele with mice expressing Cre recombinase in the germline. The colony was maintained by breeding heterozygous male mice with wild-type C57BL/6 (Charles River Laboratories). Genotyping was performed using Ready-to-go PCR beads (Amersham Pharmacia Biotech, No. 27955801) with forward primer GCCAATCAAAGTCCTGGAAGACAG and reverse primer CTGCAG-ATCATGTATACTGGTGAC.

Immunohistochemistry and in situ hybridization

For whole-mount staining, embryos were fixed in Dent's fixation (four parts methanol: one part DMSO) overnight at 4°C. Embryos were progressively rehydrated and blocked twice for 1 hour in TNB (Roche No. 11096176001). Embryos were incubated overnight at 4°C with primary antibodies (1:100) in TNB (biotinylated α-Pecam1, BD Bioscience No. 553371; rabbit α-human Collagen IV, Serotec No. 2150–0140; phospho-histone 3, Abcam No. ab5176–100). Embryos were washed, re-blocked and incubated overnight with fluorescent streptavidin or fluorescent secondary antibodies (1:400) at 4°C.

For sections, embryos were dissected and fixed in 4% PFA overnight at 4°C. Embryos were washed in 70% ethanol, stained with Eosin, dehydrated and embedded in paraffin. Immunohistochemistry was performed using the Tyramide Signal Amplification system (TSA, NEN Life Science Products, Boston, MA).

In situ hybridization has been described previously (Moyon et al., 2001a) with probes for *Dll4* (Suchting et al., 2007), *Nrp1* (Yuan et al., 2002), *Efnb2* (Moyon et al., 2001b) and *Cx40* (Mukouyama et al., 2005).

Quantitation of vascular phenotype

After Pecam1 staining, yolk sacs were mounted and imaged on a fluorescent microscope (magnification 20×). Using ImageJ, images were filtered and converted to binary images. Total vessel area was assessed by counting the number of white versus black pixels in the binary images. Network morphology was quantified using the Biologic Analyzer, a software program developed by Nicolas Elie (Centre de Morphologie Mathematiques-ARMINES, France). This program extracts the skeleton of the vascular network from binary images (S. Beucher, PhD thesis, École des Mines de Paris, 1990) (Coster and Chermant, 1985) and points where the skeleton lines intersect are counted as branchpoints (Ablameyko and Pridmore, 2000) (see Fig. S1 in the supplementary material). Segment length was assessed by dividing the total length of all skeleton lines by the number of intersections. Vessel diameter was assessed indirectly, by measuring the average area of an avascular space (hole) between vessels. Four to five images per yolk sac and a minimum of three yolk sacs per group were analyzed.

Flow assessment and creation of no-flow embryos

Breeding pairs of mice were mated overnight and the presence of a vaginal plug denoted E0.5. Embryos were collected at E8.5 and cultured as described (Jones et al., 2002), except that roller culture rather than static culture was used. For analysis of flow, embryos were collected at 5 somites and cultured for 6 or 24 hours. The yolk sac was observed under white light (10× magnification), focusing especially on the outlet of the dorsal aorta where the fastest and most visible flow is located. Embryos were time-lapsed by placing them on a heated stage after culture and images were taken with white light at a rate of ~2 Hz.

To create no-flow embryos, 3- to 4-somite stage embryos were held with No. 5 watchmaker forceps and the yolk sac and inlets to the heart were snipped on both sides of the heart using No. 55 watchmaker forceps. The embryos were then cultured for 24 hours. Most embryos recovered from the injury and had normally inflated yolk sacs (not shown) though the inlet to the heart was deformed and embryos never turned. One or two embryos per litter had deflated yolk sacs or still had blood circulation and were discarded.

Embryo injections and migration assay

Injections were performed using a pulled quartz needle filled with either 70,000 MW Texas Red dextran (Molecular Probes, No. D-1828) for angiograms or with protein solutions [Nrp1 blocking antibodies (Pan et al., 2007a) all others from R&D systems] for Nrp1 blocking experiments. For protein solutions, a small quantity of 70,000 MW Texas Red dextran was added to visualize injection. A picospritzer II (General Valve) was used to inject, the volume of the injections was set by varying the pressure until the desired amount of dye was expunged. The needle was inserted into the heart of the embryos (10 somites for angiograms, 4 somites for protein solutions), through the yolk sac. Long thin quartz needles were used to prevent damage to the yolk sac. Several pulses of solution were injected into the beating heart and dye could be visualized during injection entering the yolk sac and filling the vessels. This ensured accurate and specific dosing to only the cardiovascular system. Approximate dosing of protein solutions was calculated using an order of magnitude estimation. The dimensions of an embryo are ~1 mm×100 μm×100 μm at this stage and the density of an embryo is approximately equal to that of water. With ~10 nl of protein solution injected (4.4 mg/ml and 7.6 mg/ml for α-Nrp-1A and α-Nrp-1B, respectively), the dose is an order of magnitude of 10^3-10^4 mg of protein/kg of embryo.

In the case of the migration assay, CM-DiI (Invitrogen, C7001) dye was injected focally onto the yolk sac. Embryos (n=23 wild-type or heterozygotes, n=5 $Nrp1^{-/-}$) were cultured for 24 hours and then photographed using bright-field and fluorescent light on a Leica fluorescent dissecting microscope. Using Photoshop, the distance from the center of the injection site to the most distant fluorescent endothelial cell was measured.

Isolation of embryonic endothelial cells and quantitative RT-PCR

Embryos were collected at E9.5 or after 24 hours of culture starting at E8.5. Two to three embryos that appeared to be of the same genotype were pooled and digested with collagenase for 40 minutes. Endothelial cells were then separated using Dynabeads (Invitrogen No. 110-35) coated with Pecam1 antibody (BD Bioscience No. 553369), non-endothelial cells were collected for genotyping. Endothelial cell RNA was extracted using an RNeasy micro kit (Qiagen No. 74004). Retrotranscription was performed using MMLV reverse transcriptase and Oligo dT primers. SYBR green PCR mix (Qiagen No. 204145) and a BioRad iCycler were used to quantitate gene expression in these samples. All primers were QuantiTect Primer Assays (Qiagen). A total of six sets of two or three embryos with the correct genotype was used quantitate gene expression in each group.

RESULTS

Cardiovascular phenotype of the *Nrp1*$^{-/-}$ embryos

Neuropilin 1 (*Nrp1*) knock-out mice were generated by crossing mice harboring a conditional *Nrp1* allele with mice expressing Cre recombinase in germ cells, as described (Gu et al., 2003). Chimeras were backcrossed on a pure C57BL/6 background for more than seven generations. We examined the cardiovascular phenotype between E8.0 (4-6 somites) and E11.5.

In wild-type embryos, the earliest vessels form in the yolk sac, an extra-embryonic tissue that surrounds the developing embryo. This de novo vessel formation occurs between E8.0 and E8.5, and is known as vasculogenesis. As these early vessels connect to the embryonic heart and the heart begins to beat, the yolk sac vasculature is remodeled into a more hierarchical structure composed of arteries, capillaries and veins that can be visualized at E9.5 in freshly dissected embryos and by staining with the pan-endothelial marker Pecam1 (Fig. 1A,B). *Nrp1*-null embryos fail to undergo vascular remodeling and exhibit poorly branched, enlarged vessels throughout the yolk sac at E9.5 (Fig. 1E,F). The caliber of yolk sac vessels in *Nrp1*$^{-/-}$ embryos is similar to that of large arteries of the yolk sac in the wild-type embryos (Fig. 1B,F). As well, large avascular spaces are observed between the mutant vessels (Fig. 1E,F).

De novo formation of blood vessels in *Nrp1*-null embryos appeared identical to wild-type until E8.5 (data not shown), suggesting a possible requirement of *Nrp1* during the process of vessel remodeling but not vessel formation. To determine when the mutant phenotype became apparent, we injected fluorescently tagged dextran into the heart of normal (Fig. 1C) and mutant embryos (Fig. 1G) at 10 somites (E8.75), just after the normal onset of blood flow. The dextran highlights the vasculature of the heart, yolk sac and dorsal aortae in both wild-type and knockout embryos, indicating that lumenized vessels are present in *Nrp1*$^{-/-}$ embryos. However, the large dilated vessels and avascular spaces were already apparent in the mutant yolk sacs at this stage, indicating that the phenotype appears concomitantly with the onset of blood flow.

To quantitate the difference in the vascular phenotypes, we performed morphometric analysis (see Fig. S1 in the supplementary material) and measured total vessel coverage, the number of vessel branch points, segment length and avascular spaces between capillaries on Pecam-stained yolk sacs of wild-type and mutants (Fig. 1D,H). Before the onset of flow (E8.0, 4-6 somites), there was no statistically significant difference in overall vessel coverage, number of branchpoints or segment length between embryos of different genotypes (Fig. 1I-K). Overall vessel coverage remained similar between wild type and *Nrp1* mutants at subsequent developmental stages (data not shown). However, the number of vessel branchpoints decreased in the *Nrp1* mutant yolk sacs just after the onset of blood flow at 7-10 somites (E8.5) and at 20-25 somites (E9.5) (Fig. 1I). If the total vessel area is constant, and the number of vessel branchpoints is reduced, one expects that the length of individual vessel segments increases, which is what we observed in the *Nrp1* mutant compared with wild type (Fig. 1J). The average size of avascular areas (holes) separating capillaries increased in *Nrp1*$^{-/-}$ mutants compared with wild type both at 7-10 somites and at 20-25 somites (Fig. 1K). With constant vessel area and increased space between vessels, it follows that the individual segments must be thicker. Taken together, this quantification revealed: (1) that *Nrp1*-null yolk sac vessels show normal overall vessel coverage, but altered vascular geometry, with less branched thicker vessels separated by large avascular spaces; and (2) that these defects appear concomitantly with the onset of blood flow.

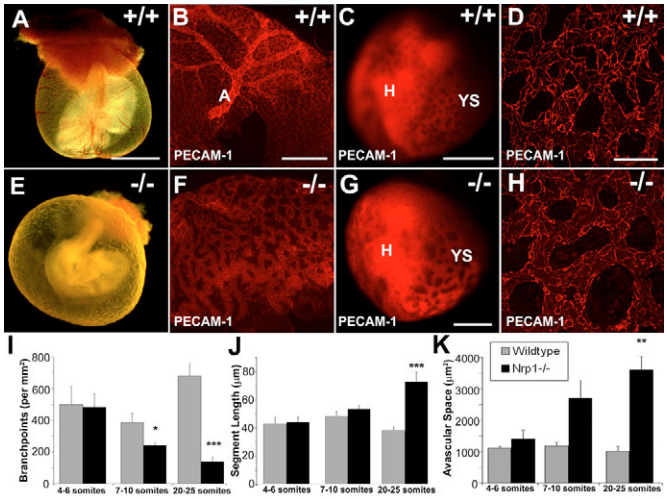

Fig. 1. Cardiovascular phenotype of *Nrp1*$^{-/-}$ embryos. Dark-field images of freshly dissected yolk sacs from E9.5 embryos with the indicated genotypes (**A**,**E**) shows defects in yolk-sac vascular remodeling that are further highlighted by Pecam1 staining of the wild-type (**B**) and mutant (**F**) yolk sacs. Angiograms at E8.5, just after the onset of plasma flow (**C**,**G**) show that vessels are lumenized in both wild-type (C) and knockout (G) embryos, but that *Nrp-1*$^{-/-}$ already show altered yolk sac vessel geometry (G). Pecam1 staining of yolk sacs (**D**,**H**) were used to quantitate the phenotype based on the number of branchpoints per mm^2 (**I**), average vessel segment length (**J**) and area of avascular spaces (**K**) at different stages of development for wild-type and knockout embryos. *P<0.05, **P<0.01, ***P<0.005; Student's two-tailed t-test. A, aorta; H, heart; YS, yolk sac. Scale bars: 1 mm in A,E; 500 μm in B,C,F,G; 100 μm in D,H.

Examination of the embryo proper between E8.5 and E9.5 showed that somite addition in *Nrp1*$^{-/-}$ embryos occurred at normal rate until E9.5 (23 to 25 somites), but ceased afterwards. A developmental delay of *Nrp1*$^{-/-}$ compared with wild-type or heterozygous littermates became apparent at E9.5. Live knockout embryos could be recovered until E10.5, but were severely growth retarded at this stage (data not shown). Taken together, we observe that *Nrp1*$^{-/-}$ embryos on the C57BL/6 background die at E10.5, consistent with previous reports of a different *Nrp1* mutant allele bred on this background (Kitsukawa et al., 1997), and exhibit vessel remodeling defects that appear concomitant with the onset of blood flow.

Nrp1$^{-/-}$ embryos exhibit abnormal blood flow

As proper blood flow is required for remodeling to occur (le Noble et al., 2004; Lucitti et al., 2007), we next investigated whether normal blood flow was present in *Nrp1*$^{-/-}$ embryos. In wild-type embryos, the heart starts beating at the 3-somite stage, initiates a period of plasma flow through the primitive vascular plexus from 3 somites until 5-6 somites, which is followed by the gradual entry of erythroblasts into circulation. Continuous circulation, where vessels are consistently filled with flowing erythroblasts, is established by ~8 somites (Lucitti et al., 2007). We investigated whether erythroblasts circulated in *Nrp1*$^{-/-}$ mutants by placing embryos at E8.5 (5-7 somites) into culture for 6 or 24 hours, as previously described (Jones et al., 2004). The embryos were removed from culture and observed under white light for circulating erythroblasts (Table 1). Using this method, we saw erythroblasts circulating in 100% of E8.5 wild-type embryos (n=12; see Movie 1 in the

Table 1. Blood flow in neuropilin mutant embryos

Embryonic stage	*Nrp1*$^{+/+}$or *Nrp1*$^{+/-}$	*Nrp1*$^{-/-}$
E8.5 (10 somites)	100% continuous circulation (*n*=12)	14% continuous circulation, 86% oscillatory circulation (*n*=7)
E9.5	100% normal circulation (*n*=13)	100% absence of circulation (*n*=4)

supplementary material) and 100% of E9.5 wild-type embryos (*n*=13). By contrast, normal circulation was not observed at either stage in embryos lacking *Nrp1*. In E8.5 mutant embryos, erythroblasts could only be seen oscillating in place (Table 1, see Movie 2 in the supplementary material) and continuous movement of erythroblasts through the early vascular plexus was never observed. By E9.5, no erythroblast motion was observed in the mutant embryos (*n*=4) and circulation had completely arrested. Thus, *Nrp1* homozygous mutants can initiate heart contraction and plasma flow (Fig. 1G), but fail to initiate erythroblast circulation.

To investigate possible causes of the defective blood flow, we sectioned and stained wild-type and mutant embryos at E8.5 and E9.5 (Fig. 2). *Nrp1* expression in arteries of the E8.5 (10-somite stage) embryo and yolk sac vessels (Fig. 2A), detected by in situ hybridization, provided a possible causative explanation for the vascular remodeling defect. In addition, *Nrp1* stained the atrial compartment of the heart (Fig. 2A). Using RT-PCR, we could

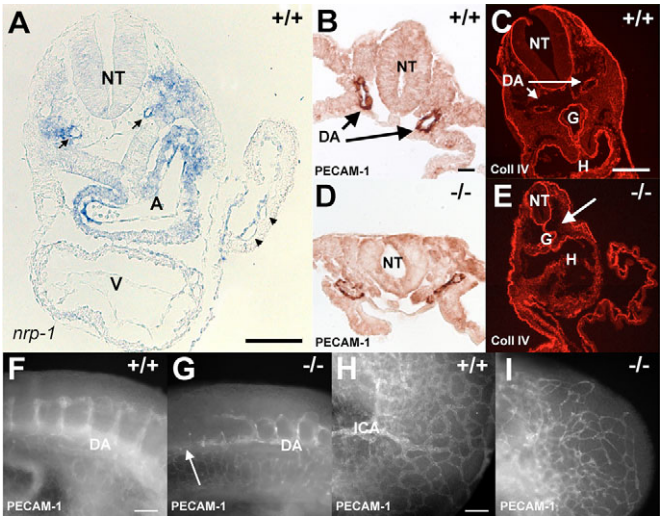

Fig. 2. Investigating causes of defective flow in *Nrp1*$^{-/-}$ embryos. (**A**) In situ hybridization with an *Nrp1* antisense riboprobe on a section from a wild-type embryo at 10 somites shows expression in the atrium (marked A) and not the ventricle (marked V), as well as expression in the dorsal aortae (arrows) and yolk-sac vessels (arrowheads). (**B**,**D**) Serial sections of E8.5 wild-type (B) and mutant (D) embryos stained for Pecam1 show that dorsal aortae (DA) are present and lumenized in both cases, though often collapsed in the mutant (D). (**C**) By E9.5, collagen IV staining highlights the dorsal aortae (DA), gut (G) and heart (H) of wild-type embryos. (**E**) In mutant embryos, one or both dorsal aortae are often missing (arrow). (**F**,**G**) Intersomitic vessel sprouting is visible in E9.5 wild-type embryos stained for Pecam1 (F) but is delayed in mutant embryos (G) and also shows the absent dorsal aorta (arrow). (**H**,**I**) The cephalic region of E9.5 wild-type embryos shows an extensive vasculature (H) that is also present in the mutant embryos (I); however, the vasculature of the mutants is more sparse and many vessels do not appear to be lumenized. The internal carotid artery (ICA) has started forming in the wild-type (H) but is lacking in the mutant (I). NT, neural tube. Scale bars: 50 μm in A,B,D; 100 μm in F-I; 200 μm in C,E.

detect *Nrp1* expression in the heart as early as 4 somites (*n*=4), and this expression was sustained at 7 somites (*n*=4) and 10 somites (*n*=4).

Lack of cardiac *Nrp1* expression could cause the observed blood flow defects, as oscillatory flow has previously been seen in embryos that specifically lack the atrial component of heart contractions (Lucitti et al., 2007). The heart of *Nrp1*-null embryos underwent proper looping at E8.5; however, the pericardial sac of the mutant embryos was consistently enlarged by E10.5 (*n*=7) and no trabeculation was observed from E9.5 onwards. At E8.5, the endocardial lining stained positively for Pecam1 and was present in both wild-type and mutant embryos (data not shown). The size of the heart also appeared to be normal. Therefore, the heart appeared morphologically normal at 10 somites when flow problems could already be observed. To determine whether heart function was normal in the *Nrp1*-null embryos, we placed embryos at the 6-somite stage into culture for 6 hours and observed the form of the heart contraction. Heart contractions initiate at the base of the heart and move anteriorly in both wild-type and *Nrp1* knockout embryos (*n*=8 for wild type and *n*=3 for mutant). Heart rate also did not differ significantly between wild-type and mutant (51±4.5 bpm and 40±5.7 bpm, respectively; see Movies 1, 2 in the supplementary material). We therefore conclude that heart function is also grossly normal in the mutant embryos, although more subtle defects could not be detected with this method.

As cardiac function appeared grossly normal, we next looked at whether the vasculature of the embryo proper had formed normally. Pecam1 staining at E8.5 showed that both dorsal aortae were present in wild-type (Fig. 2B) and mutant embryos (Fig. 2D). The diameter of these vessels appeared normal throughout the embryo, but *Nrp1*$^{-/-}$ vessels were often collapsed, perhaps impeding blood flow and circulation, although the dextran injections showed that vessels were lumenized at this stage (Fig. 1G). At E9.5, collagen IV staining on sections from wild-type embryos revealed two dorsal aortae on either side of the neural tube (Fig. 2C). One or both of these vessels, at the level of the heart, were missing in *Nrp1* mutant embryos (Fig. 2E,G; Fig. 4B), though they were generally still present at the caudal end of the embryo. E9.5 *Nrp1* mutant embryos also showed delayed vessel sprouting into the intersomitic regions when compared with wild-type (Fig. 2F,G), though sprouts that progressed far enough interconnected as in wild-type. The cephalic vascular plexus developed in *Nrp1*$^{-/-}$ embryos, although the vessels were thinner and sparser than in normal embryos and did not appear to be lumenized (Fig. 2H,I). Smooth muscle cells, visualized with α-SMA staining, surrounded the major vessels of the embryo in wild-type embryos, but were not present either in the head or trunk region of homozygous mutant embryos (data not shown).

Separating the role of blood flow from Nrp1 function

As the histological and functional analysis of the cardiovascular system in *Nrp1*-null embryos did not reveal a major defect in the mutant heart or vessels of the embryo proper, the yolk sac vascular phenotype in *Nrp1*$^{-/-}$ mice could be due to defective flow causing

defective vessel remodeling or vice versa. We therefore sought to differentiate primary effects caused by lack of *Nrp1* from secondary defects caused by abnormal flow.

We suspected a direct role of Nrp1 signaling during the formation of yolk sac vessels, because the vascular phenotype in the yolk sac of *Nrp1*-null embryos was not the same as published for embryos that completely lack flow, such as the *Ncx1*$^{-/-}$ embryos (Wakimoto et al., 2000), or embryos that exhibit only oscillatory flow, such as the *Mlc2a*$^{-/-}$ embryos that we have previously analyzed (Lucitti et al., 2007). We therefore created embryos that completely lacked flow in order to compare the vasculature of wild-type 'no-flow' embryos with those of *Nrp1* mutants. By placing wild-type and mutant embryos into the same no-flow mode, the comparison of the phenotypes reflects only the role of *Nrp1* and not normal versus abnormal or absent flow. We created no-flow embryos by snipping the inlet to the heart in 4-somite embryos (see Materials and methods), a stage when the heart has started beating but erythroblast circulation has not initiated. These embryos are then cultured for 24 hours using whole embryo roller culture. The presence or absence of flow is evaluated after culture at a stage when circulation of erythroblasts is normally evident. The vasculature is then stained using antibodies to Pecam1 and the number of vessel branch points, vessel segment length and avascular spaces are quantitated.

In wild-type embryos with normal flow, key aspects of vascular remodeling were apparent after culture, such as changes in branch angle and the formation of large vessels in the yolk sac. These large, regularly branched vessels are separated by capillary regions (Fig. 3A). As observed in freshly dissected embryos (Fig. 1F), cultured *Nrp1* mutants fail to undergo remodeling and to create a hierarchical branching system (Fig. 3A). Though the overall vascular coverage was not affected in *Nrp1* mutants (n=12 for wild-type, n=10 for mutant, data not shown), the yolk sac vessels showed decreased branching, increased segment length and large spaces separating vessels. The difference in vessel diameter between wild-type and mutant embryos was also apparent in sections (inlays, Fig. 3A).

Comparing embryos in the no-flow environment, we found that wild-type and knockout embryos did not show the same vascular phenotype (Fig. 3A). In wild-type no-flow embryos, large vessels never formed and the entire vasculature remained reminiscent of the capillary regions of the yolk sac with blood flow. Vessel branching was decreased (Fig. 3B); however, no change in segment length or in the area of avascular spaces was present compared with embryos experiencing normal flow (Fig. 3C,D). Cultured no-flow *Nrp1*$^{-/-}$ embryos also showed decreased branching (Fig. 3B), but in addition showed increased segment length (Fig. 3C) and increased area of avascular spaces (Fig. 3D), similar to the vascular phenotype of *Nrp1*$^{-/-}$ embryos in normal flow conditions and in striking contrast to the phenotype of wild-type no-flow embryos. Thus, all aspects of the *Nrp1*$^{-/-}$ yolk sac vessel phenotype develop in no-flow culture conditions, indicating that the phenotype is due to loss of Nrp1 function.

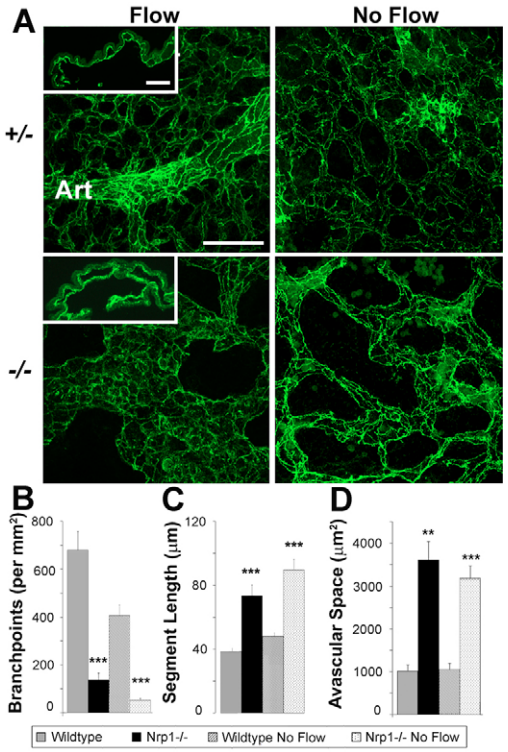

Fig. 3. Separating the role of blood flow from *Nrp1* function. (**A**) Pecam1 staining of yolk sacs from cultured heterozygote and mutant embryos in both flow and no-flow conditions, as indicated. In heterozygote embryos with flow, a large remodeled artery (Art) is visible. Heterozygote embryos without flow fail to remodel capillaries into large vessels. Insets show collagen IV staining on sections from E9.5 yolk sacs that also highlight the large vessel diameters in *Nrp1*$^{-/-}$ yolk sacs compared with wild type. (**B-D**) *Nrp1*$^{-/-}$ vessels, with or without flow, show decreased branching (B), increased vessel segment length (C) and increased avascular spaces (D). $^{**}P<0.01$; $^{***}P<0.005$; Student's two-tailed t-test. Scale bar: 100 μm.

Blocking Nrp1 function reproduces the *Nrp1*$^{-/-}$ yolk sac vessel phenotype

Having determined that loss of Nrp1 function, rather than disturbed blood flow, was responsible for the altered vascular geometry in the yolk sac of *Nrp1*$^{-/-}$ embryos, we reasoned that blocking Nrp1 function in wild-type embryos should reproduce the vascular phenotype observed in *Nrp1*-null mutants. We used antibodies that specifically block either Sema3A or VEGFA binding to Nrp1 (Pan et al., 2007a). Treated embryos were cultured for 24 hours, Pecam1 stained (Fig. 4A-D), and yolk sac vessel branching and avascular spaces were quantified (Fig. 4E-G). To optimize protein delivery to the yolk sac, we first compared direct addition of protein to the medium of cultured embryos and intracardiac injection of protein solution, using $VEGF_{120}$, which is expected to increase vessel coverage. We found that intracardiac injection was preferable as $VEGF_{120}$ could not diffuse across the yolk sac when added directly to the medium (data not shown). Injection of $VEGF_{120}$ led to an increase in the vascular coverage (from 74.1±1.1% to 85.9±1.1%) such that most of the yolk sac stained positive for Pecam1 (Fig. 4B). Having optimized protein delivery, we analyzed the effects of intracardiac injection of Nrp1 blocking antibodies (Pan et al., 2007a). Anti-Nrp1A antibody blocks Sema3A binding and anti-Nrp1B is specific for the VEGF binding domain of Nrp1, though both prevent receptor dimerization with Vegfr2. Both antibodies were capable of decreasing vessel branching and increasing segment length (Fig. 4C-F). Anti-Nrp-1A had no effect on the area of avascular regions, but anti-Nrp1B was able to create large avascular regions similar to those seen in the *Nrp1*$^{-/-}$ embryos (Fig. 4C,D,G). Injection of both antibodies together did not create a synergistic effect on branching, and effects on avascular spaces were similar to the ones seen with anti-Nrp1B alone (Fig. 4G). Attempts at blocking Nrp1 function by injection of soluble Nrp1, which should sequester Nrp1 ligands including $VEGF_{165}$ (Gagnon et al., 2000), had no effect

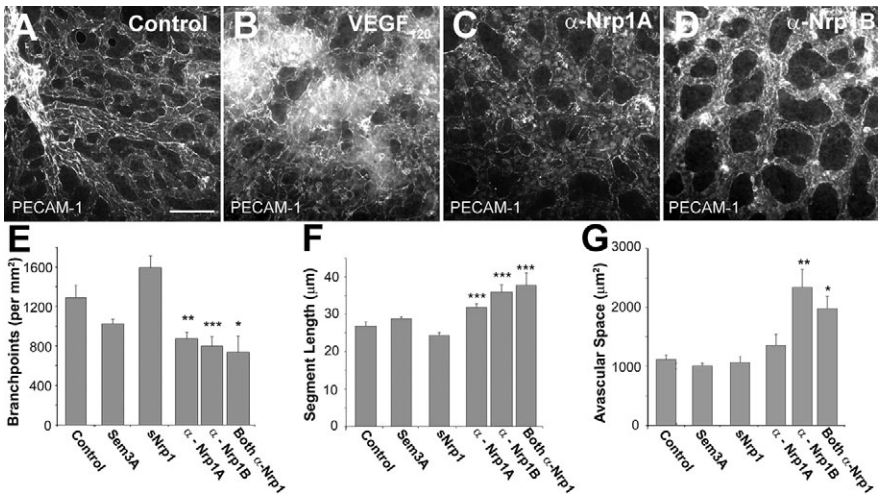

Fig. 4. Blocking Nrp1 function reproduces the *Nrp1*$^{-/-}$ yolk sac vessel phenotype. Wild-type embryos from a CD1 background were treated with various proteins by intracardiac injection followed by whole-embryo culture. (**A-D**) Subsequent to culture, the vasculature was fixed and stained for Pecam1. (**E-G**) The images were quantified for vascular morphology. Untreated embryos showed remodeling, typical of E9.5 embryos (A). $VEGF_{120}$ injection caused an increase in overall vascular coverage (B). Injection of antibodies against Nrp1, which are reported to block Sema3A binding (C) and VEGF binding (D) to Nrp1 (Pan et al., 2007b), were both effective at decreasing the number of branchpoints and increasing vessel segment length as seen in the *Nrp-1*$^{-/-}$ embryos (E,F). Injection of both antibodies did not show a synergistic effect on the number of branchpoints. Only antibodies against the VEGF-binding domain of Nrp1 were capable of increasing average area of avascular space, as seen in *Nrp1*$^{-/-}$ embryos (G). Injection of Sem3A and Nrp1 had no statistically significant effect on capillary geometry (E-G). *P<0.05, **P<0.01, ***P<0.005; Student's two-tailed t-test. Scale bars: 100 μm.

on yolk sac vasculature (Fig. 4E-G). Injection of the Nrp1 ligand Sema3A, which had previously been shown to compete with $VEGF_{165}$ for Nrp1 binding (Miao et al., 1999), also had no significant effects (Fig. 4E-G), consistent with recent data showing directly that Sema3A and VEGF do not compete for binding to Nrp1 (Appleton et al., 2007), and that Sema3A mutant mice lack an observable vascular phenotype (Vieira et al., 2007). Though no effects were observed in these injection experiments, it was not possible to assess whether larger quantities of protein could have elicited a response. The embryo and its network of blood vessels are small at this stage and limit how much protein solution can be injected into the embryo without causing injury. However, inhibition of Nrp1 function with a blocking antibody to the VEGF binding domain in wild-type embryos could clearly reproduce the altered vascular geometry observed in *Nrp1* knockout yolk sacs, confirming that this aspect of the phenotype was due to loss of Nrp1 function and not to altered blood flow.

Replication, sprouting, regression and migration in *Nrp1*$^{-/-}$ vessels

Nrp1 has been implicated in sprouting (Gerhardt et al., 2004), migration (Pan et al., 2007b) and proliferation of endothelial cells (Soker et al., 1998). We therefore investigated how endothelial cell behavior in the yolk sac was different between mutant and wild-type embryos. Endothelial cell replication was assessed at various developmental stages in wild-type and mutant embryo yolk sacs using phospho-histone H3 and Pecam1 double-staining (Fig. 5A). No significant difference in the number of dividing endothelial cells was observed between the two groups at all stages investigated (n=3-4 embryos per group with five images per embryo). Replication of smooth muscle cells and of total cells in the yolk sac at E9.5 was also similar between *Nrp1* knockouts and wild type (not shown). Taken together with the similar total vessel coverage observed in wild-type and knockouts, these results indicate that endothelial replication is unlikely to account for the observed yolk sac vessel defects in *Nrp1* knockouts. The sprouting and regression of vessels was assessed by counting the number of Pecam1 stained endothelial cells extending into avascular spaces of the yolk sac, such that they formed dead-ended vessels (unconnected extensions). No differences were observed between the different groups and the presence or absence of flow did not affect this measure (Fig. 5B).

Endothelial cell migration was assessed by focal injection of a lipophilic carbocyanine dye (DiI) using a picospritzer into a capillary region of the yolk sac (red arrow, Fig. 5D,E) followed by culture to allow marked cells to migrate. Regions where the fluorescence is continuous from cell to cell indicate endothelial cells migrating away from the site of injections (Fig. 5F,G). In wild-type embryos, marked cells migrate but remain confined within proximity to the injection site (Fig. 5C,D,F, n=23). *Nrp1* knockout DiI-positive cells migrate along the abnormally formed yolk sac capillaries and are found at greater distances from the injection area than wild-type cells (Fig. 5C,E,G, n=5). Quantification of the distance of cell migration confirmed that endothelial cells migrated further away from the injection site in *Nrp1*$^{-/-}$ compared with wild-type yolk sacs (Fig. 5C), indicating that they exhibit abnormal migration.

Defective arterial differentiation in *Nrp1*$^{-/-}$ embryos is not flow related

Previous reports have indicated that arterial differentiation is defective in endothelial-specific *Nrp1* knockouts (Mukouyama et al., 2005). Though arterial identity is established before the onset of flow, the expression of arterial markers remains plastic and changes with the flow that endothelial cells are exposed to. If an embryonic artery is ligated to create an environment where the vessels experience venous flow, expression of markers such as ephrin B2

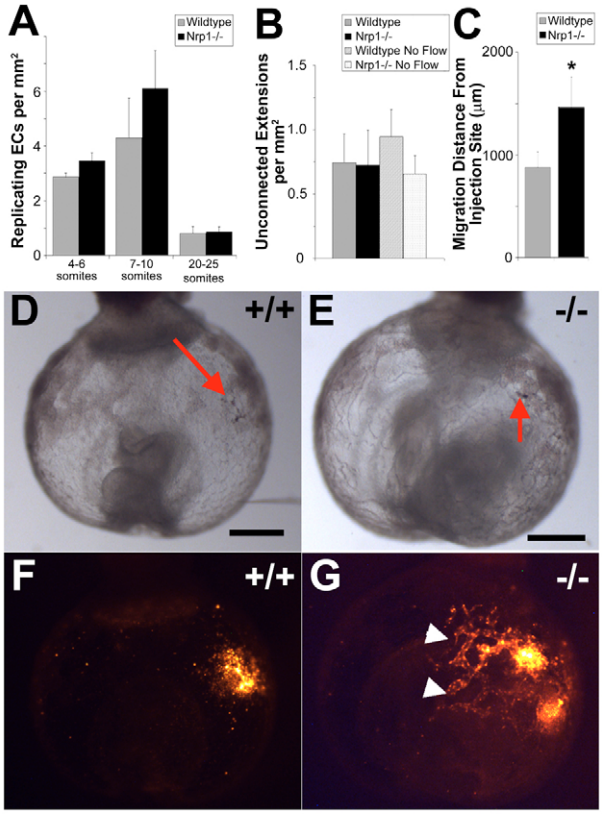

Fig. 5. Replication, sprouting and migration in *Nrp1*$^{-/-}$ yolk sacs. (**A**) Endothelial replication was quantitated using double staining with phospho-histone 3 and Pecam1 at different stages of development. No statistically significant difference was seen at any of the stages examined. (**B**) The number of Pecam1-positive unconnected segments extending into avascular spaces, which may represent sprouts or regressing vessels, was assessed from images of the yolk sac at E9.5. No significant differences were observed between the different groups. (**C-G**) Endothelial cell migration was assessed by focal injection of cell tracker CM-DiI into a capillary region of the yolk sac followed by quantification of the maximum migration distance per embryo (C). The initial injection site can be observed in the white light images (red arrows, D,E). Endothelial cells did not migrate very far away from the site of injection in wild-type embryos (F) but were seen migrating longer distances along existing capillaries for knockout embryos (arrowheads, G). *P<0.05, Student's two tailed t-test. Scale bar: 1 mm.

will be downregulated and expression of venous markers will be upregulated (le Noble et al., 2004). Other groups have also shown that endothelial cells change their gene expression depending on the waveform of the flow that they are exposed to (Blackman et al., 2002). We therefore investigated whether changes in arterial-venous gene expression in *Nrp1* mutants were created by the abnormal flow present in these embryos.

We examined the expression pattern of arterial markers delta-like 4 (*Dll4*), connexin 40 (*Cx40*; Gja5 – Mouse Genome Informatics) and ephrin B2 (*Efnb2*) by in situ hybridization in both wild-type and mutant embryos (Fig. 6A-F). At E9.5, *Dll4* was expressed in the common atrial chamber of the heart and in the dorsal aorta of wild-type or heterozygous embryos (Fig. 6A). In *Nrp1*$^{-/-}$ embryos (Fig. 6B), we observed expression both in the common atrial chamber and in the dorsal aorta (when present, red arrow denotes missing second dorsal aorta). *Cx40* expression can be seen specifically in the common atrial chamber and in the dorsal aorta for wild-type embryos (Fig. 6C). This expression is completely lacking in *Nrp1*$^{-/-}$ embryos (Fig. 6D). *Efnb2* was expressed in the somites, neural tube, the dual dorsal aortae and the vitelline artery of wild type (Fig. 6E). *Nrp1*$^{-/-}$ embryos showed normal *Efnb2* expression in somites and neural tube, as well as staining in the endothelium of the dorsal aorta, but labeling of the vitelline artery was reduced compared with wild-type or heterozygous littermates (Fig. 6F).

To further explore differences in gene expression between *Nrp1*$^{-/-}$ and wild-type embryos, we used quantitative RT-PCR. Endothelial cells were isolated from two or three embryos using Dynabeads coated with antibodies against Pecam1 (see Materials and methods). From this cell population, RNA was extracted and analyzed. To rule out effects of flow induced gene expression, we also tested endothelial cell gene expression in wild-type and mutant embryos that lacked flow. In all, six sets of two or three embryos were analyzed per group. The relative expression levels were measured for 11 cardiovascular genes (Fig. 6G): four pan-endothelial, four arterial and three venous. These were normalized to three housekeeping genes, β-actin, α-tubulin and *Gapdh*. Most genes showed no significant difference in expression level between wild-type, *Nrp1*$^{-/-}$, no-flow wild type and no-flow knockout (*Hif1a*, *Vegfr2*, VE-cadherin (*Cdh5* – Mouse Genome Informatics), *Dll4*, *Nrp2* and *Ephb4*). Expression of *Vegfa* and *Unc5b* was altered in endothelial cells of *Nrp1* mutants compared with wild type (Fig. 6G). Stopping flow, however, eliminated the difference between wild-type and mutant, indicating that no difference is seen when observed on the same flow background. *COUP-TF2* (*Nr2f2* – Mouse Genome Informatics) levels were unaffected by the *Nrp1* mutation but were decreased in no-flow conditions (Fig. 6G). In contrast to these genes, expression of the arterial markers *Efnb2* and *Cx40* was specifically downregulated in *Nrp1* mutants (Fig. 6G), as reported previously in endothelial-specific *Nrp1* knockouts (Mukouyama et al., 2005). The decrease in *Efnb2* levels was modest, confirming the in situ hybridization results, indicating that not all vessels lost *Efnb2* expression, while expression of *Cx40* was strongly decreased in *Nrp1* mutants. Downregulation of *Efnb2* and *Cx40* was not flow related but specific to loss of *Nrp1*, as the difference was also present between no-flow wild-type and knockout embryos.

DISCUSSION

Vessel remodeling and flow defects in *Nrp1*$^{-/-}$ mutants

In this work, we study the role of Nrp1 in cardiovascular development. A previous study of *Nrp1*$^{-/-}$ embryos showed that embryonic lethality occurred at E10.5 on a C57BL/6 background, but only at E13.5 on a CD-1 background (Kitsukawa et al., 1997). Cardiovascular defects in *Nrp1* mutants were so far only analyzed in the CD-1 mutants (Kawasaki et al., 1999) and in endothelial-specific conditional mutants, which also die at E13.5 (Gerhardt et al., 2004; Gu et al., 2003; Mukouyama et al., 2005). In agreement with the initial report (Kitsukawa et al., 1997), our extensive analysis of an *Nrp1* mutant allele bred on C57BL/6 showed lethality at E10.5. In fact, these *Nrp1*$^{-/-}$ embryos show arrest of all cardiovascular progress one day after cardiovascular function normally begins. The heart has looped but no trabeculations form. The dorsal aortae form normally at E8.5 but are regressing by E9.5, and smooth muscle cells do not surround large vessels. Yolk sac vessels fail to remodel into arteries and veins, show reduced branching, diameter increase and enlarged avascular spaces. The embryo begins to appear necrotic by E9.5 and is slowly resorbed by E11.5. Analysis of flow patterns showed that normal flow was never

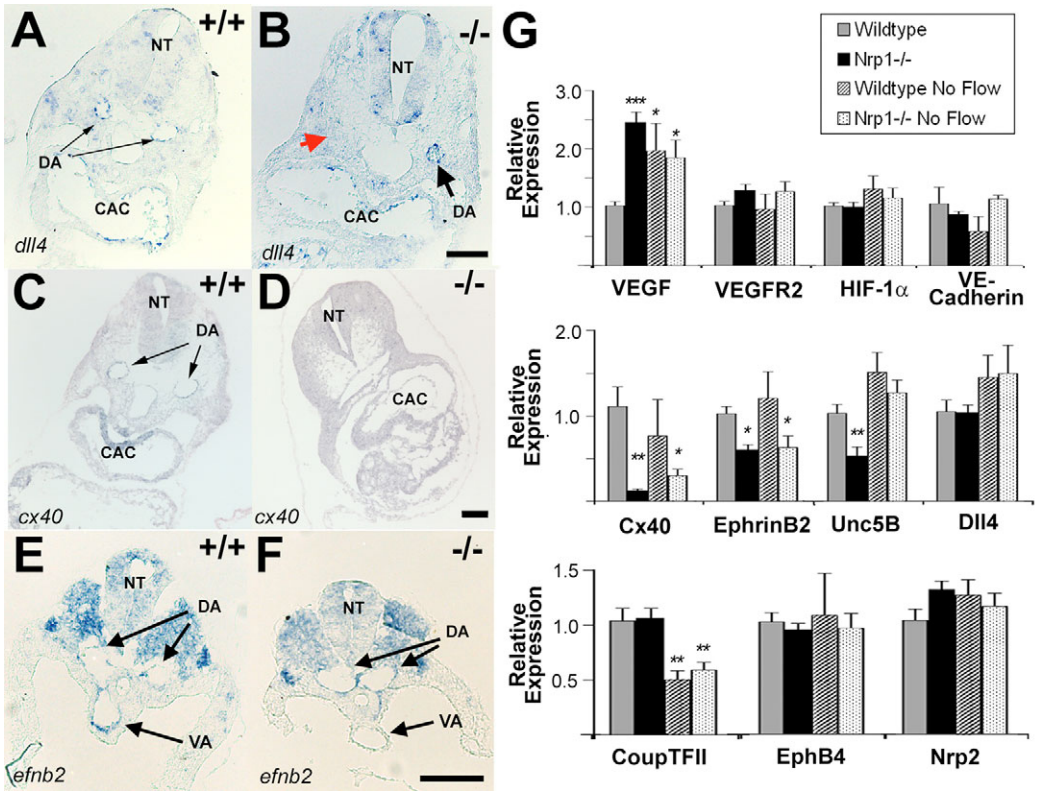

Fig. 6. Arterial venous gene expression in *Nrp1*$^{-/-}$ embryos. (**A-F**) Serial sections were stained by in situ hybridization for *Dll4* (A,B), *Cx40* (C,D) and *Efnb2* (E,F) in both wild-type (A,C,E) and *Nrp1* knockout embryos (B,D,F) at 20 somites. Images show the common atrial chamber (CAC), the vitelline artery (VA) and the dorsal aortae (DA) at either the level of the heart (A-D) or at the caudal end of the embryo (E,F). (B) Red arrow indicates a missing dorsal aorta in the *Nrp1*$^{-/-}$ embryo; the remaining dorsal aorta still expresses *Dll4*. (D) *Cx40* expression is absent in *Nrp1*$^{-/-}$ embryos. (F) Normal expression of *Efbn2* is present in dorsal aorta and somites of *Nrp1*$^{-/-}$ embryos, but lacking in the vitelline artery. (**G**) Levels of gene expression were measured from isolated endothelial cells, either pooled wild-type/heterozygous (denoted wild-type) or knockout, both with and without blood flow for 11 cardiovascular genes: four pan-endothelial genes, four arterial genes and three venous genes. Gene expression was normalized to three housekeeping genes: α-tubulin, β-actin and *Gapdh*. Expression of *Cx40* and *Efbn2* in *Nrp1*$^{-/-}$ is downregulated compared with wild type, regardless of flow environment. **P*<0.05, ***P*<0.01, ****P*<0.005; Student's two-tailed *t*-test. Scale bars: 100 μm.

observed in *Nrp1* null mutants. As vascular defects appear concomitantly with blood flow defects, they could be secondary to the flow defects or caused by the *Nrp1* mutation.

Though blood flow was aberrant in the *Nrp1*$^{-/-}$ embryos, no major cardiovascular defects were observed in the embryo proper when flow defects first became visible. Heart development and function were normal and all the major vessels of the embryo were present and lumenized at E8.5. More-subtle changes in heart function cannot be measured at these young stages and remain a possible cause of flow insufficiencies. However, the defects in the yolk-sac vasculature may actually cause the abnormal flow. When the heart begins to contract at 3 somites, a period of plasma flow is initiated (Lucitti et al., 2007). As heart development continues, plasma flow increases and eventually carries erythroblasts into circulation. Enlarged yolk sac vessels would require a larger pump (or stronger heart) than normal to create an equivalent velocity of plasma flow in the vessels given the laws of conservation of mass. If the plasma is not flowing fast enough, then the erythroblasts cannot circulate. *Nrp1*$^{-/-}$ embryos on a CD1 background are not resorbed until E13.5 (Kitsukawa et al., 1997), although they show aberrant yolk sac vessel geometry similar to the one described here (Kawasaki et al., 1999). We speculate that the difference in the stage at which the mutant embryos die in these two backgrounds could be due to slightly increased embryo growth rate, heart contractility and blood flow in CD1 versus C57BL/6 embryos, which would be sufficient to initiate blood flow but still encounter altered vascular geometry and eventually fail to establish proper circulation.

Separating genetic and flow defects in *Nrp1*$^{-/-}$ mutants

Abnormal flow makes analysis of mouse mutants challenging as it becomes an issue of whether flow or loss of signaling function cause the mutant phenotype. In N-cadherin (Cdh2 – Mouse Genome Informatics) mutants, cardiac-specific rescue of gene expression was sufficient to rescue flow and cardiovascular defects observed in null mutants (Luo et al., 2001). As no obvious cardiac defects were detected in the *Nrp1*-null mutants, we did not attempt cardiac-specific re-expression of *Nrp1*. To identify aspects of the phenotype caused by loss of *Nrp1* function, we sought to compare embryos in the same flow environment and decided to analyze embryos in the absence of flow. We find that the geometry of the capillary plexus in *Nrp1*-null embryos in a no-flow environment is altered such that there are fewer branch points, longer vessel segments and larger avascular spaces between vessels, indicative of increased vessel diameter. This phenotype is seen in both no-flow and untreated *Nrp1*-null embryos and therefore not related to flow. This method

allowed us to identify aspects of the phenotype that are purely due to loss of Nrp1 function. The relative simplicity of the method, when compared with transgenic rescue experiments, makes it easily applicable to analysis of numerous mouse mutants for genes involved in cardiovascular development in which abnormal flow is suspected.

Formation of defective capillary geometry in *Nrp1*$^{-/-}$ mutants

To confirm that altered yolk sac vessel geometry in *Nrp1*$^{-/-}$ mutants was due to loss of Nrp1 function rather than to abnormal flow, we injected wild-type embryos with blocking antibodies specific to either the Sema3A or the VEGF-binding domains of Nrp1. Both antibodies decreased yolk-sac vessel branching, but only the Nrp1B VEGF blocking antibody led to phenocopy of all aspects of the *Nrp1*$^{-/-}$ vascular morphology. Previous studies have shown that both antibodies reduce VEGF-driven endothelial cell migration and sprouting angiogenesis in various in vitro and in vivo models, with anti-Nrp1B being slightly more potent than anti-Nrp1A (Pan et al., 2007a). Both antibodies disrupt complex formation of Nrp1 and Vegfr2, suggesting that both inhibit VEGF-driven motility via disruption of complex formation and downstream signaling events. Our results agree with these findings, as inhibiting the Sema3A-binding domain showed a small effect on vascular morphology, while injection of antibodies that block the VEGF-binding domain mimicked multiple aspects of the *Nrp1*$^{-/-}$ phenotype. Furthermore, injection of antibody blocking VEGF binding to Nrp1 could induce the *Nrp1*$^{-/-}$ capillary phenotype in wild-type embryos experiencing normal flow. These experiments therefore clearly identify the aberrant vascular geometry as a primary defect caused by loss of Nrp1 signaling.

Endothelial replication was similar between wild-type and mutants and could not account for the altered *Nrp1*$^{-/-}$ yolk sac vessel geometry. Thus, loss of Nrp1 function does not influence endothelial cell replication in vivo, confirming previous findings with antibodies blocking VEGF or Sema3A binding to Nrp1, which failed to inhibit VEGF-driven endothelial proliferation in vitro (Pan et al., 2007a). We also found no differences in sprouting/regression between wild type and *Nrp1*$^{-/-}$ mutants. However, the number of Pecam-positive endothelial cells extending into avascular yolk sac areas was very low (less than 1 per mm^2). Time-lapse studies in early quail embryos have shown that formation of the vascular plexus involves endothelial cell migration along existing endothelial cord structures as well as sprouting (Rupp et al., 2003). Although sprouting appeared to be an important mechanism to generate new vascular cords, only a small fraction of endothelial cells was shown to exhibit protrusive behavior over the period of recording (Perryn et al., 2008). Thus, sprout formation in yolk sac vessels may be missed in fixed samples. We can therefore not rule out altered sprouting or regression of yolk sac endothelial cells as a potential mechanism accounting for the altered vascular morphology of *Nrp1*-null yolk sacs.

We found significant differences in the pattern of endothelial migration between wild-type and *Nrp1*$^{-/-}$ mutants. Focal DiI injections showed that *Nrp1* knockout cells are found at greater distances from the injection area than wild-type cells. This observation was surprising, as one might have expected migration of *Nrp1*$^{-/-}$ cells to be decreased. However, the mutant cells appeared to migrate along existing endothelial cell cords and were never seen leaving existing vessels. Thus, rather than exhibiting a general block of migration, it appears that *Nrp1* mutant cells fail to migrate in the proper direction, most probably via loss of VEGF signaling. Migration along existing capillaries has been shown to require cell-cell rather than extracellular matrix interactions (Rupp et al., 2003), suggesting that interactions between endothelial Nrp1 and matrix-bound VEGF may be disrupted in the mutant mice. Loss of Nrp1 function may thus perturb binding of extracellular matrix-bound $VEGF_{164}$, complex formation with Vegfr2 and downstream signaling, leading to inhibition of directional migration and vessel branching, without affecting other aspects of endothelial function such as proliferation. Such a mechanism would explain the reduction in branchpoints and larger vessel diameters as the same numbers of endothelial cells are creating fewer vessels. Alternatively, as qPCR analysis has shown that *Nrp1* mutant endothelial cells express elevated *Vegf* mRNA levels, increases in VEGF signaling through Vegfr2 may cause the increase in endothelial migration we observe. We find this model unlikely, however, as *Vegf* levels in cultured no-flow wild-type or *Nrp1*$^{-/-}$ mutants are similar, yet their vascular phenotypes differ. Furthermore, injection of antibodies blocking VEGF binding to Nrp1 into wild-type embryos with normal flow and presumably unaltered VEGF levels can reproduce altered capillary geometry.

Endothelial gene regulation by Nrp1

As the maintenance of expression of arterial markers requires flow (le Noble et al., 2004), we investigated whether changes in arterial-venous gene expression in *Nrp1* mutants were created by the abnormal flow present in these embryos. We found that expression levels of arterial markers *Cx40* and *Efnb2* were decreased in *Nrp1* mutants compared with wild-type embryos. For *Efnb2*, this change appears to be linked to extra-embryonic vessels, as highlighted by the loss of expression in the vitelline artery. These two genes were previously reported downregulated in endothelial-specific conditional *Nrp1* knockout embryos (Mukouyama et al., 2005); however, the effect of flow was not analyzed. Wild-type embryos cultured in no-flow conditions showed no changes in the expression levels of these two genes, indicating that the decrease was specific for the *Nrp1* mutation and not secondary to altered blood flow, thus confirming and extending previous reports (Mukouyama et al., 2005).

This work was supported by grants from INSERM, Ministère de la Recherche (ANR-PCOD, ANR Neuroscience, ANR blanche), ARC (3124), Institut de France (Cino del Duca) and the European Community (LSHG-CT-2004-503573). We thank Y. Mukouyama for providing the Cx40 probe. E.A.V.J. was supported by the Foundation Lefoulon-Delalande and a Marie Curie Action Fellowship (IIF 022006). R.J.W. is an employee of Genentech and the antibodies provided by him where developed by Genentech. All other authors have nothing to disclose.

Supplementary material

Supplementary material for this article is available at
http://dev.biologists.org/cgi/content/full/135/14/2479/DC1

References

Ablameyko, S. and Pridmore, T. P. (2000). Machine Interpretation of Line Drawing Images. Secaucus, NJ: Springer-Verlag.

Appleton, B. A., Wu, P., Maloney, J., Yin, J., Liang, W. C., Stawicki, S., Mortara, K., Bowman, K. K., Elliott, J. M., Desmarais, W. et al. (2007). Structural studies of neuropilin/antibody complexes provide insights into semaphorin and VEGF binding. *EMBO J.* **26**, 4902-4912.

Blackman, B. R., Garcia-Cardena, G. and Gimbrone, M. A., Jr (2002). A new in vitro model to evaluate differential responses of endothelial cells to simulated arterial shear stress waveforms. *J. Biomech. Eng.* **124**, 397-407.

Chapman, W. B. (1918). The effect of the heart-beat upon the development of the vascular system in the chick. *Am. J. Anat.* **23**, 175-203.

Clark, E. R. (1918). Studies on the growth of blood vessels in the tail of frog. *Am. J. Anat.* **23**, 37-88.

Coster, M. and Chermant, J. L. (1985). Precis d'Analyse d'Images. Paris: Les Editions du CNRS.

Gagnon, M. L., Bielenberg, D. R., Gechtman, Z., Miao, H. Q., Takashima, S., Soker, S. and Klagsbrun, M. (2000). Identification of a natural soluble neuropilin-1 that binds vascular endothelial growth factor: *In vivo* expression and antitumor activity. *Proc. Natl. Acad. Sci. USA* **97**, 2573-2578.

Gerhardt, H., Ruhrberg, C., Abramsson, A., Fujisawa, H., Shima, D. and Betsholtz, C. (2004). Neuropilin-1 is required for endothelial tip cell guidance in the developing central nervous system. *Dev. Dyn.* **231**, 503-509.

Grazioli, A., Alves, C. S., Konstantopoulos, K. and Yang, J. T. (2006). Defective blood vessel development and pericyte/pvSMC distribution in alpha 4 integrin-deficient mouse embryos. *Dev. Biol.* **293**, 165-177.

Gu, C., Rodriguez, E. R., Reimert, D. V., Shu, T., Fritzsch, B., Richards, L. J., Kolodkin, A. L. and Ginty, D. D. (2003). Neuropilin-1 conveys semaphorin and VEGF signaling during neural and cardiovascular development. *Dev. Cell* **5**, 45-57.

He, Z. and Tessier-Lavigne, M. (1997). Neuropilin is a receptor for the axonal chemorepellent Semaphorin III. *Cell* **90**, 739-751.

Jones, E. A., Crotty, D., Kulesa, P. M., Waters, C. W., Baron, M. H., Fraser, S. E. and Dickinson, M. E. (2002). Dynamic in vivo imaging of postimplantation mammalian embryos using whole embryo culture. *Genesis* **34**, 228-235

Jones, E. A., Baron, M. H., Fraser, S. E. and Dickinson, M. E. (2004). Measuring hemodynamic changes during mammalian development. *Am. J. Physiol. Heart Circ. Physiol.* **287**, H1561-H1569.

Kawasaki, T., Kitsukawa, T., Bekku, Y., Matsuda, Y., Sanbo, M., Yagi, T. and Fujisawa, H. (1999). A requirement for neuropilin-1 in embryonic vessel formation. *Development* **126**, 4895-4902.

Kitsukawa, T., Shimizu, M., Sanbo, M., Hirata, T., Taniguchi, M., Bekku, Y., Yagi, T. and Fujisawa, H. (1997). Neuropilin-semaphorin III/D-mediated chemorepulsive signals play a crucial role in peripheral nerve projection in mice. *Neuron* **19**, 995-1005.

Kolodkin, A. L., Levengood, D. V., Rowe, E. G., Tai, Y. T., Giger, R. J. and Ginty, D. D. (1997). Neuropilin is a semaphorin III receptor. *Cell* **90**, 753-762.

le, Noble, F., Moyon, D., Pardanaud, L., Yuan, L., Djonov, V., Matthijsen, R., Breant, C., Fleury, V. and Eichmann, A. (2004). Flow regulates arterial-venous differentiation in the chick embryo yolk sac. *Development* **131**, 361-375.

Lucitti, J. L., Jones, E. A., Huang, C., Chen, J., Fraser, S. E. and Dickinson, M. E. (2007). Vascular remodeling of the mouse yolk sac requires hemodynamic force. *Development* **134**, 3317-3326.

Luo, Y., Ferreira-Cornwell, M., Baldwin, H., Kostetskii, I., Lenox, J., Lieberman, M. and Radice, G. (2001). Rescuing the N-cadherin knockout by cardiac-specific expression of N- or E-cadherin. *Development* **128**, 459-469.

May, S. R., Stewart, N. J., Chang, W. and Peterson, A. S. (2004). A Titin mutation defines roles for circulation in endothelial morphogenesis. *Dev. Biol.* **270**, 31-46.

Meeson, A., Palmer, M., Calfon, M. and Lang, R. (1996). A relationship between apoptosis and flow during programmed capillary regression is revealed by vital analysis. *Development* **122**, 3929-3938.

Miao, H. Q., Soker, S., Feiner, L., Alonso, J. L., Raper, J. A. and Klagsbrun, M. (1999). Neuropilin-1 mediates collapsin-1/semaphorin III inhibition of endothelial cell motility: functional competition of collapsin-1 and vascular endothelial growth factor-165. *J. Cell Biol.* **146**, 233-242.

Moyon, D., Pardanaud, L., Yuan, L., Breant, C. and Eichmann, A. (2001a). Plasticity of endothelial cells during arterial-venous differentiation in the avian embryo. *Development* **128**, 3359-3370.

Moyon, D., Pardanaud, L., Yuan, L., Breant, C. and Eichmann, A. (2001b). Selective expression of angiopoietin 1 and 2 in mesenchymal cells surrounding veins and arteries of the avian embryo. *Mech. Dev.* **106**, 133-136.

Mukouyama, Y. S., Gerber, H. P., Ferrara, N., Gu, C. and Anderson, D. J. (2005). Peripheral nerve-derived VEGF promotes arterial differentiation via neuropilin 1-mediated positive feedback. *Development* **132**, 941-952.

Pan, Q., Chanthery, Y., Liang, W. C., Stawicki, S., Mak, J., Rathore, N., Tong, R. K., Kowalski, J., Yee, S. F., Pacheco, G. et al. (2007a). Blocking neuropilin-1 function has an additive effect with anti-VEGF to inhibit tumor growth. *Cancer Cell* **11**, 53-67.

Pan, Q., Chanthery, Y., Wu, Y., Rahtore, N., Tong, R. K., Peale, F., Bagri, A., Tessier-Lavigne, M., Koch, A. W. and Watts, R. J. (2007b). Neuropilin-1 binds to VEGF121 and regulates endothelial cell migration and sprouting. *J. Biol. Chem.* **282**, 24049-24056.

Perryn, E. D., Czirok, A. and Little, C. D. (2008). Vascular sprout formation entails tissue deformations and VE-cadherin-dependent cell-autonomous motility. *Dev. Biol.* **313**, 545-555.

Rupp, P. A., Czirok, A. and Little, C. D. (2003). Novel approaches for the study of vascular assembly and morphogenesis in avian embryos. *Trends Cardiovasc. Med.* **13**, 283-288.

Soker, S., Takashima, S., Miao, H. Q., Neufeld, G. and Klagsbrun, M. (1998). Neuropilin-1 is expressed by endothelial and tumor cells as an isoform-specific receptor for vascular endothelial growth factor. *Cell* **92**, 735-745.

Suchting, S., Freitas, C., le Noble, F., Benedito, R., Breant, C., Duarte, A. and Eichmann, A. (2007). The Notch ligand Delta-like 4 negatively regulates endothelial tip cell formation and vessel branching. *Proc. Natl. Acad. Sci. USA* **104**, 3225-3230.

Thoma, R. (1893). Untersuchungen über die Histogenese und Histomechanikdes Gefässsytems. Stuttgart: Ferdinand Enke.

Vieira, J. M., Schwarz, Q. and Ruhrberg, C. (2007). Selective requirements for NRP-1 ligands during neurovascular patterning. *Development* **134**, 1833-1843.

Wakimoto, K., Kobayashi, K., Kuro, O. M., Yao, A., Iwamoto, T., Yanaka, N., Kita, S., Nishida, A., Azuma, S., Toyoda, Y. et al. (2000). Targeted disruption of Na^+/Ca^{2+} exchanger gene leads to cardiomyocyte apoptosis and defects in heartbeat. *J. Biol. Chem.* **275**, 36991-36998.

Yuan, L., Moyon, D., Pardanaud, L., Breant, C., Karkkainen, M. J., Alitalo, K. and Eichmann, A. (2002). Abnormal lymphatic vessel development in neuropilin 2 mutant mice. *Development* **129**, 4797-4806.